NANOSTRUCTURED Fe_2O_3 THICK FILM AS AN ETHANOL SENSOR

N. K. Pawar [1], D. D. Kajale [2], G. E. Patil [2], V. G. Wagh [3], V. B. Gaikwad [4], M. K. Deore [5] and G. H. Jain [4]*

[1] Department of Physics, K.A.A.N.M. Sonanwane Arts, Commerce and Science College, Satana, 423 301 India

[2] Materials Research Lab., Arts, Commerce and Science College, Nandgaon 423 106, India

[3] Department of Physics, K.V.N. Naik Arts, Commerce & Science College, Nashik 422 002, India

[4] Materials Research Lab., KTHM College, Nashik 422 002, India

[5] Department of Physics, Arts, Commerce and Science College, Ozar Mig, 422 206 India

*Corresponding Author: gotanjain@rediffmail.com

Submitted: Mar. 24, 2012 ***Accepted: May 9, 2012*** ***Published: June 1, 2012***

Abstract- Thick films of AR Grade nano Fe_2O_3 material with n-type semiconducting properties were prepared and tested for their gas sensing performances. Thick films of the materials were prepared by screen printing technique. The gas sensing performance was studied using static gas sensing system. The material was tested for various gases such as CO, CO_2, NH_3, Cl_2, H_2, LPG, ethanol and H_2S. The nano Fe_2O_3 film showed maximum sensitivity to ethanol gas at 350 ^oC temperature at 250 ppm concentration with short response time and large recovery time. Physical and structural properties of the film material were studied by SEM, TEM, XRD and UV spectroscopy.

Index terms: Nano Fe_2O_3, Ethanol, Gas sensor, Sensitivity.

I. INTRODUCTION

In recent years considerable attention has been focused on use of metal oxide semiconductors for the purpose of gas sensing application. Iron oxide, metal oxide semiconducting material, can exist in various forms such as α-Fe_2O_3, γ-Fe_2O_3 and Fe_3O_4. The gas sensing properties of α & γ forms are still not established and contrasts are available in Iron oxide literature [1, 2]. Some papers attribute to gas–sensing properties of γ-Fe_2O_3 and Fe_3O_4 rather than to α-Fe_2O_3. The α-Fe_2O_3 form has been recognized as having minimal gas-sensing response [1] It has been reported that the thermal stability of the γ-Fe_2O_3 limits its use as gas sensor [2] Iron titanium oxide solid solutions have shown response to ethanol [3]. Some report says α-Fe_2O_3, the most stable iron oxide with n–type semiconducting properties under ambient conditions, is extensively used as gas sensor, catalysts [4, 5-9]. In metal oxide semiconductor thick film gas sensor, surface structure of the film and surface to volume ratio play very important role in sensing performance. In present work nano Fe_2O_3, being smaller in size, was especially studied to observe the effect of change in surface to volume ratio on the gas sensing performance of the material. As it is known a specific area is sharply increased with decrease of grain size. A high specific surface area and comparability of grain size (D) with the thickness surface charge layer can take great advantage for the development of high–sensitive gas sensors [10]. It is known that the surface of nano structure with high surface to volume ratio is very unstable and it easily adsorbs foreign molecules for stabilization [9, 10]. Structural factor for nanoscaled material is complicated conception and apart from size, crystallite shape, nanoscopic structure, crystallographic orientation of nanocrystallites planes forming gas sensing surface affect sensing performance of the sensing material [11].

II. EXPERIMENTAL

The AR grade nano Fe_2O_3 powder was taken and the thixotropic paste was formulated for printing the films. Thixotropic paste was formulated by mixing nano Fe_2O_3 powder with the organic binder. The inorganic to organic part was kept 75:25 in formulating the paste. Thick films of the material were prepared by screen printing technique. The prepared thick films were

fired at 550^{o}C for 30 min for removal of organic binder. The thickness of the film was measured by weight difference method.

Gas-sensing measurements were carried out by the static gas-sensing system Figure 1 [12] in which the testing material film was mounted on the stand with electric heater in the glass chamber. The temperature was maintained by automatic temperature controller. The adequate voltage was given through electrical contacts to the film.

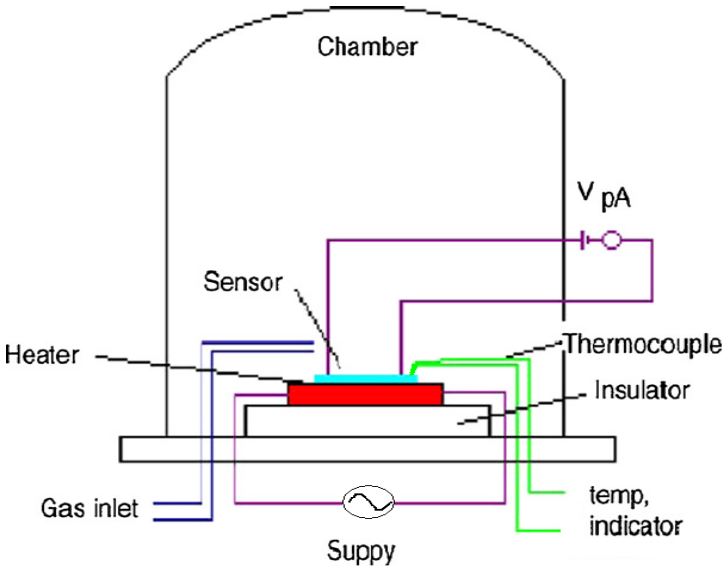

Figure 1. Schematic of static gas sensing system

Known volume of the gas was injected in the chamber through the syringe. The change in the resistance of the film on exposure to the gas was noted by observing corresponding change in the current passing through the pico-ammeter connected in series with the testing film. The sensor was fixed on to a sample holder with heater. Working temperature was determined with the help of thermocouple attached to the sensor. The different concentrations of sensing gases were maintained in the test chamber. The temperature was kept constant during each measurement. The sensor response, change in current passing through test material, was measured by pico-ammeter.

III. RESULTS AND DISCUSSION

a. Structural characterization

i. Thickness measurement

The thickness of the film prepared by screen printing technique was measured by the weight difference method [13]**.** The substrate was weighed before deposition (screen printing) of the film. After depositing the material on the substrate, the film was dried and sintered and again its weight was taken. The weight difference, density of the material and the area of the film were used to identify the thickness of the film

Thickness of the film t= M/A. ρ ……………………………………….(1)

Where M is difference between weight of the substrate after and before deposition of the film, A is the area of the film deposited in cm^3 and ρ is the density of the material deposited in $gmcm^{-3}$. The thickness of the film observed was 27 µm.

ii. XRD

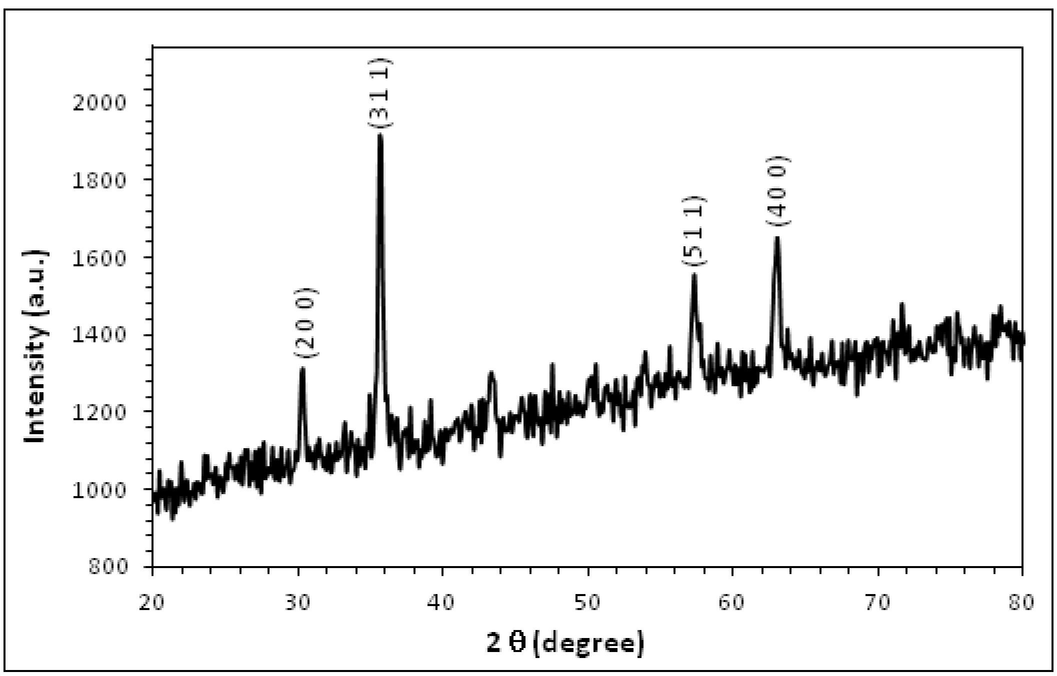

Figure 2. XRD image of nano Fe_2O_3.

The structural properties of the film was studied using X-ray diffractometer (Bruker D 8 Advance, France) with Cu Kα radiation of wavelength 1.5404 Å. Figure 2 shows the XRD of the nano Fe_2O_3. The peaks with the plane (2 0 0), (3 1 1), (5 1 1), (4 0 0) and all other found to be exactly matched with the standard peaks with corresponding planes values. XRD of the material was taken to assure the state of the material. The material found was Maghemite-C with cubic-system, primitive lattice. Well defined peaks for Fe_2O_3 were seen in the diffractogram. The XRD found well matched with the file no.39-1346 of JCPDS data and all peaks matched well with the JCPDS data. The d spacing from the XRD was calculated it also found well matched with the standard value value. The standard value for d spacing for (3 1 1) plane is 2.52 and the calculated value from the XRD was found 2.5177. This indicates the phase of the material matches well with standard material.

iii. Optical / absorption properties of nano Fe_2O_3 thick films by UV spectroscopy

Optical absorption spectrum of the sample was recorded from UV- VIS spectrometer (Shimadzu Japan Model 2450). The variation in the absorbance with respect to wave length is shown in the graph in Figure 3.

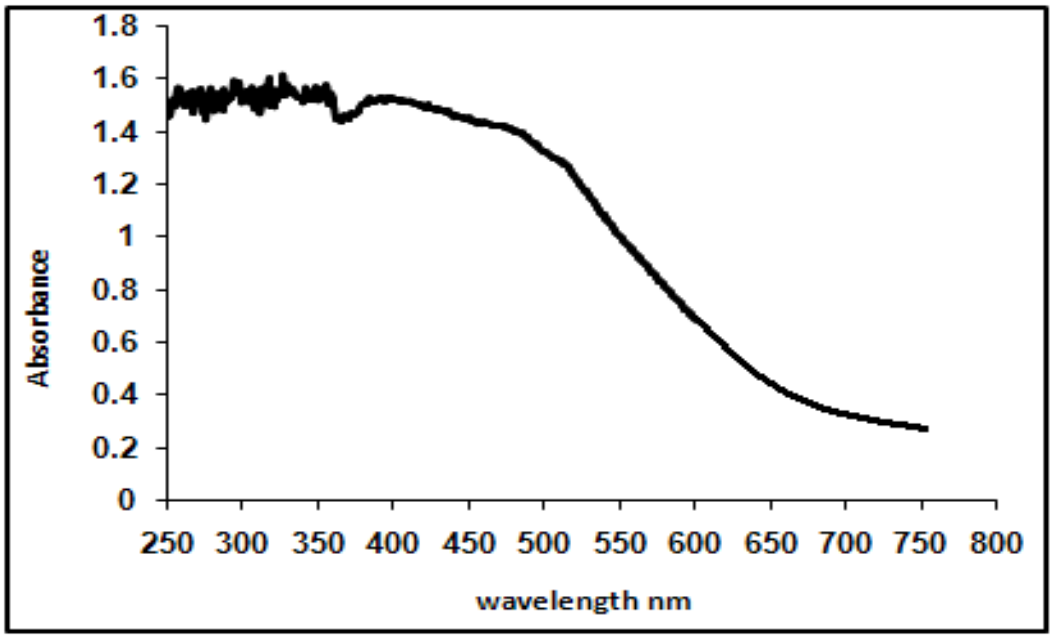

Figure 3. Optical absorbance of nano Fe_2O_3 by UV spectroscopy.

Figure 4 shows the graph of $(\alpha h\nu)^2$ versus energy hν. From the slope of the graph the energy gap of Fe_2O_3 observed is 2.1 ev.

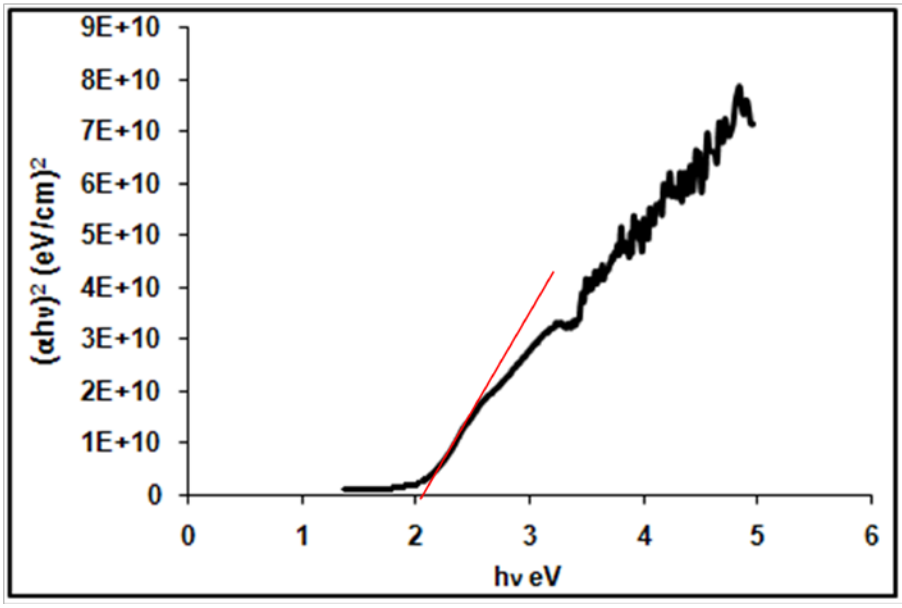

Figure 4. Plot of $(\alpha h\nu)^2$ versus hv.

iv. SEM

For examining the surface morphology of the film and percentage of constituent particles in the film the scanning electron micrographs along with energy dispersive analysis were taken using JOEL 2300 model (Japan).

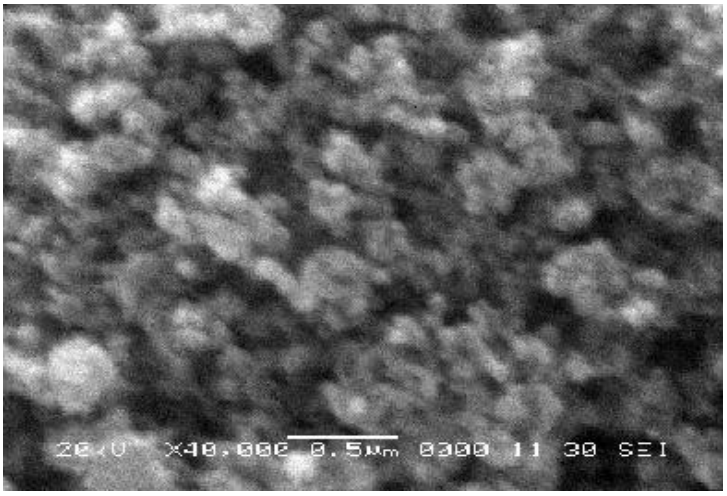

Figure 5. SEM image of the functional material nano Fe_2O_3.

Figure 5 shows typical SEM micrograph of the of nano Fe_2O_3 thick film prepared by screen printing technique the SEM image depicts the surface morphology of the film. The film shows small circular shaped grains of the Fe_2O_3 along with the porous nature of the film. This porosity, which causes increase in surface to volume ratio eventually increase in interaction with gas molecule, is beneficial for gas sensing properties of the film.

v. Quantitative Analysis:

Table 1 shows the elemental analysis which clearly depicts the percentage of O and Fe present in the film. No noticeable amount of impurities is found in the film material.

Table 1: Elemental analysis of functional material using EDAX.

Elements	**mass%**
O	7.85
Fe	92.15
Total	100.00

vi. TEM

In order to verify the nano size and crystal structure of the material TEM images of the material were taken. TEM images were recorded from transmission electron microscope (Philips CM 200 make with point resolution 2.8Å). TEM image shows the nano structure of the material and surface morphology of the sensing layer. In TEM sharp regular angular faces were seen indication that the material was well crystallized.

Figure 6 shows the nano particles observed in the TEM image. Particles of size ranging from 51.29nm to 43.62nm are observed in TEM image. The average size of the particle observed is 25.69 nm.

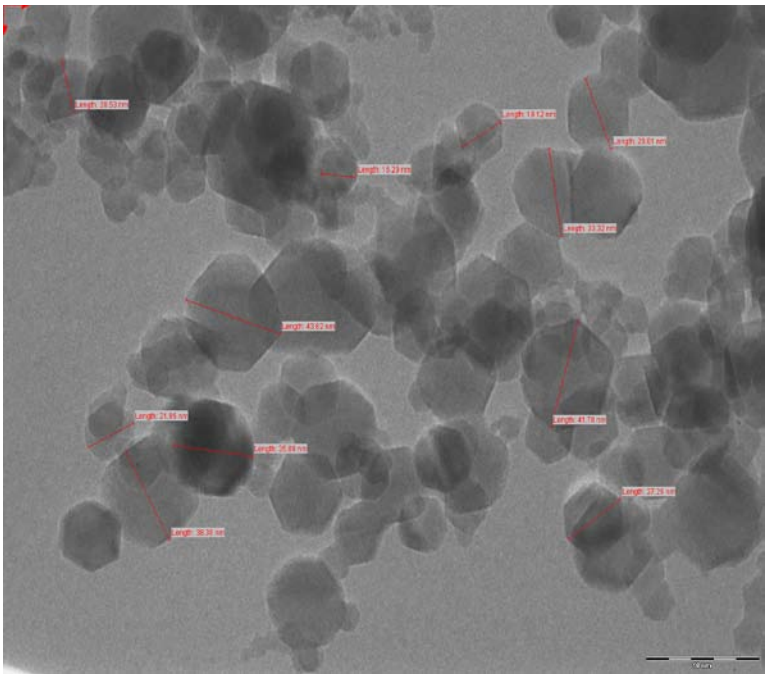

Figure 6. TEM image showing the nano sized particles of nano Fe_2O_3.

Figure 7 shows a selected area electron diffraction pattern of Fe_2O_3 nanoparticle, the observed ring pattern reveals the crystallne structre of the material. The d spacing observed in the difrraction pattern are in consistance with the standard values and the values obtained from XRD.

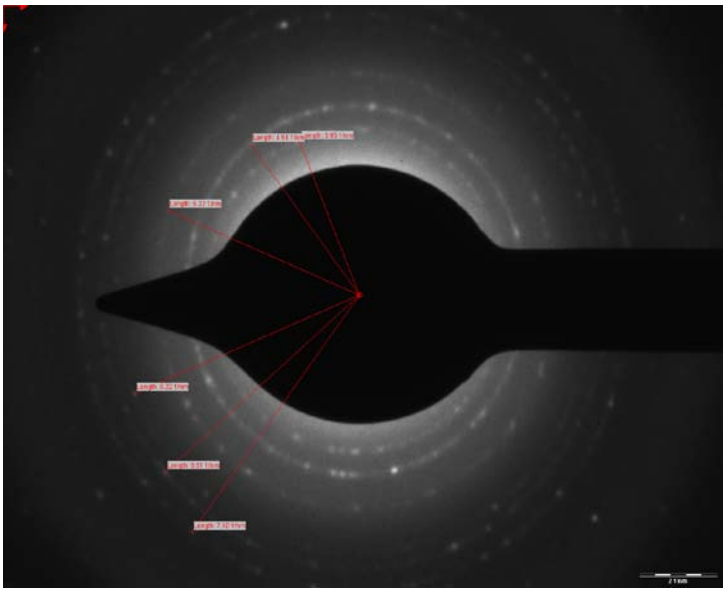

Figure 7. Selected area electron diffraction pattern of nano Fe_2O_3.

b. Electrical properties

i. I-V Characteristics

Figure 8 shows the current voltage relationship of the film under testing. It is well known that there is strong corelation between electronic transport and structural characteristics of the films. During the heat treatment the structure of the film may cahnge eventually the I-V relation may vary. From the graph, as the nature is almost linear, it is clear that the contacts on the film were ohmic in nature.in nature.

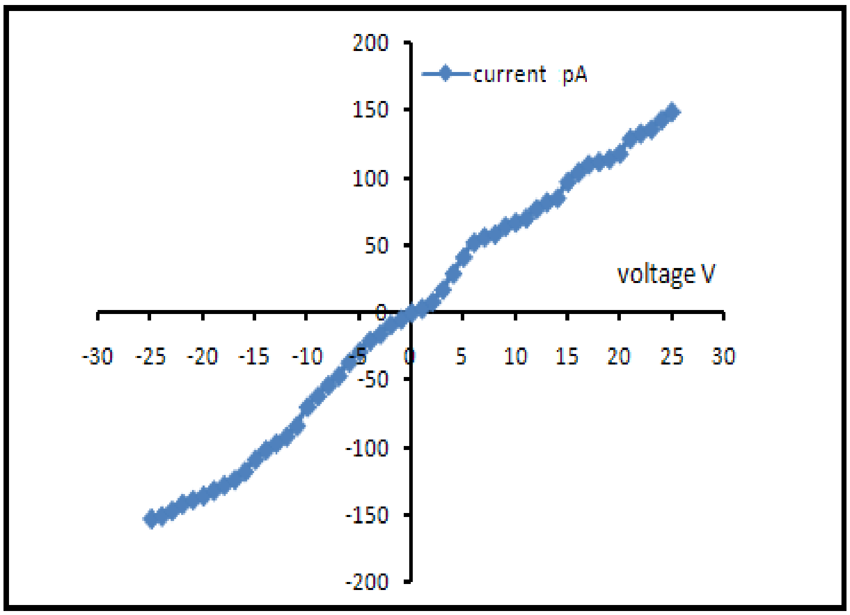

Figure 8. I-V characteristics of Fe_2O_3 nanoparticles thick film.

ii. Temperature dependent electrical conductivity of the film

Temperature dependent electrical conductivity of the film is shown in the Figure 9. It is observed that the conductivity of the film almost increases linearly with the increase in temperature. This increase in electrical conductivity is attributed to improvement of charge density and semiconducting nature of the film. Temperature dependence of electrical conductivity (σ) of the sample is expressed in terms of the Arrhenius model and is given by the relation

$$\sigma = \sigma_0 \exp (Ea/ kT) \quad \ldots\ldots(2)$$

σ_0 is pre-exponential factor , Ea is the activation energy, k is Boltzmann constant and T is the absolute temperature.

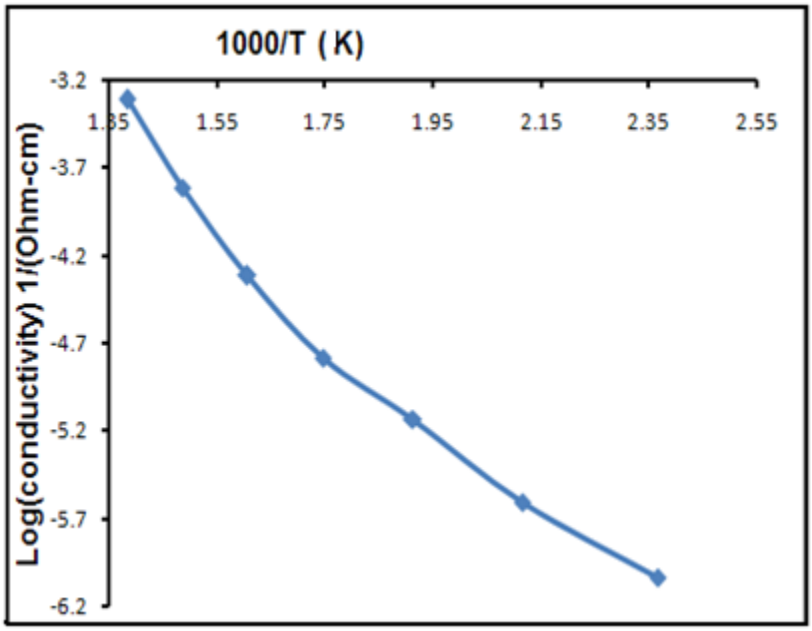

Figure 9. Temperature dependent electrical conductivity.

c. Gas response measurement

The Fe_2O_3 sample was tested for various gases at different temperatures ranging from 150 ^oC to 450 ^oC. The variation in gas concentration was studied by observing the variation in current Ia (air) and current Ig (testing gas). The sensitivity to the particular gas at particular temperature was calculated by the relation [14-15]

$$\text{Sensitivity} = (\text{Ig-Ia})/\text{Ia} \quad \ldots\ldots\ldots\ldots\ldots\ldots \quad \mathbf{(3)}$$

i. Gas sensing properties

Figure 10 shows the variation in the gas response at different temperature for various gases. It also reveals that the selectivity of ethanol gas as compared to other gases. The nano Fe_2O_3 film showed maximum sensitivity (180) to ethanol gas at 350 ^oC temperature, whereas response to other gases was very low as compared to response to ethanol.

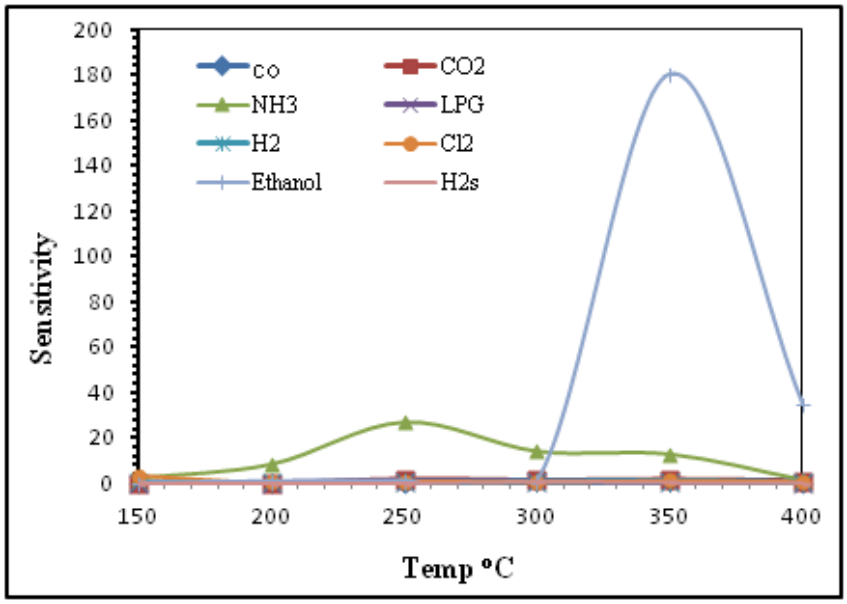

Figure 10. Sensitivity performance of nano Fe_2O_3 film to all tested gases.

ii. Selectivity of the sensor

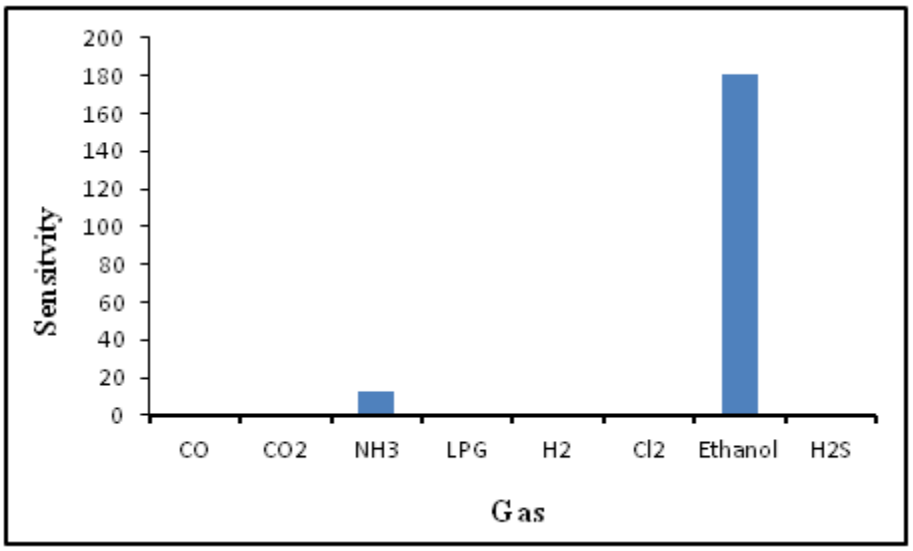

Figure 11. Selectivity to various gases at 350 ^{o}C.

Selectivity to the gas indicates that sensing performance of the film to the test gases at particular temperature. Figure 11 shows the selectivity of the sensor. In present work the test material showed maximum sensitivity to ethanol gas at 350 ^{o}C while at the same temperature the

sensitivity response to all other gases tested was very low as compared to ethanol gas. The sensor found highly selective to ethanol at 350 ^{o}C as compared to other gases.

iii. Long term stability of the sensor

Working life of the sensor is one of the most important parameter for its practical application. The long term stability test of the sensor was conducted to obsereve the variation in its sensitivity reponse corresponding to its aging period. After every five days time span the response of the film was tested. The process of tesiting was carried for 70 days. The observed change in sensitivty was decrease in sensitvity. The sensitivity was dropped from 180 to 168. Figure 12 shows the variation in the sensitivity with respect to the period in days.

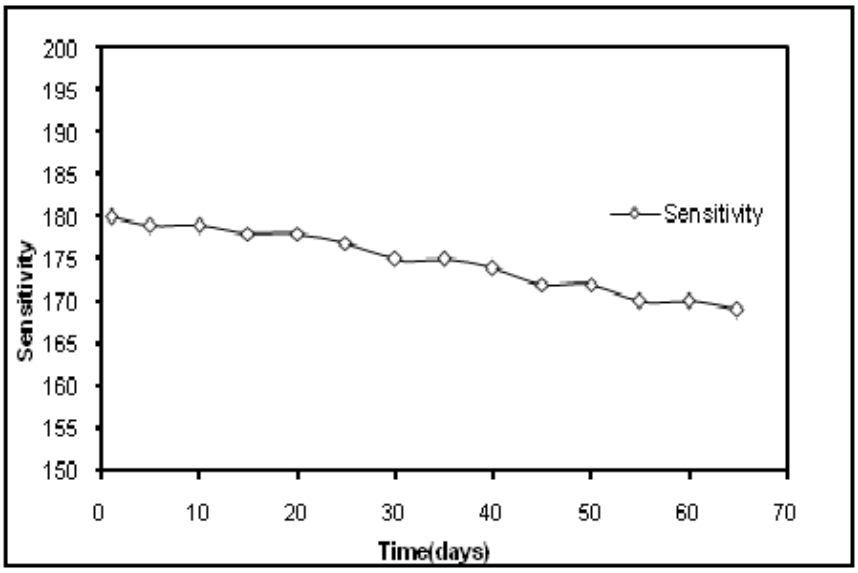

Figure 12. Long term stability.

iv. Response and recovery times

These are the important parameters for designing sensor for the desired operation. The response time is defined as the time taken for the sensor to attain 90 % of the maximum change in resistance on exposure to the test gas and the recovery time is defined as the time taken by the sensor to get back to 10 % of the value of its resistance at the time of maximum resistance.

In present work the response and recovery times are defined as the times required for a sensor to reach 90 % of its full response. From Figure.13, the response and recovery time for the

sensing response can be clearly observed. The response and recovery times for ethanol gas at 350 ^{o}C at 250 ppm gas-concentration were found to be 7 s and 32 s.

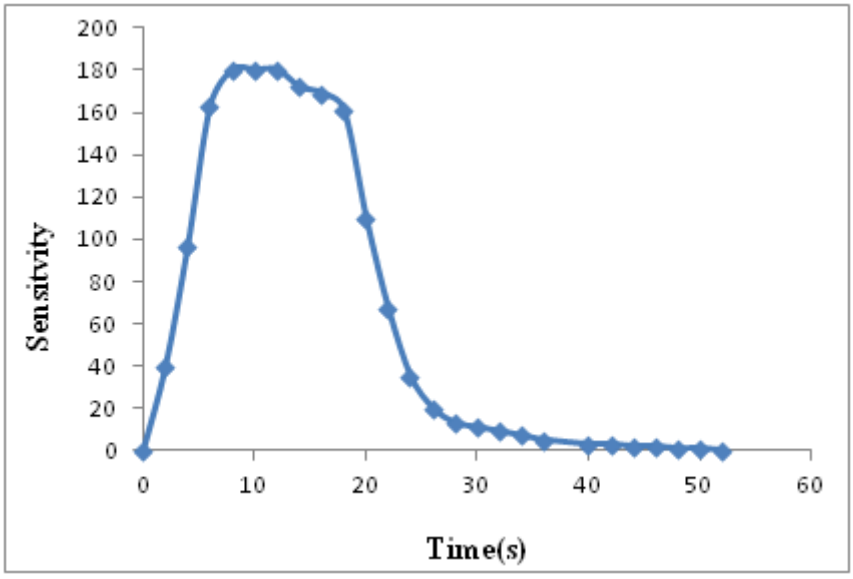

Figure 13. Response and recovery profile.

IV. GAS SENSING MECHANISM

a. Electrical conduction mechanism of n-type material and ethanol

Figure 14 shows mechanism of electrical conduction due to the gas sensing in n-type material [16-18].

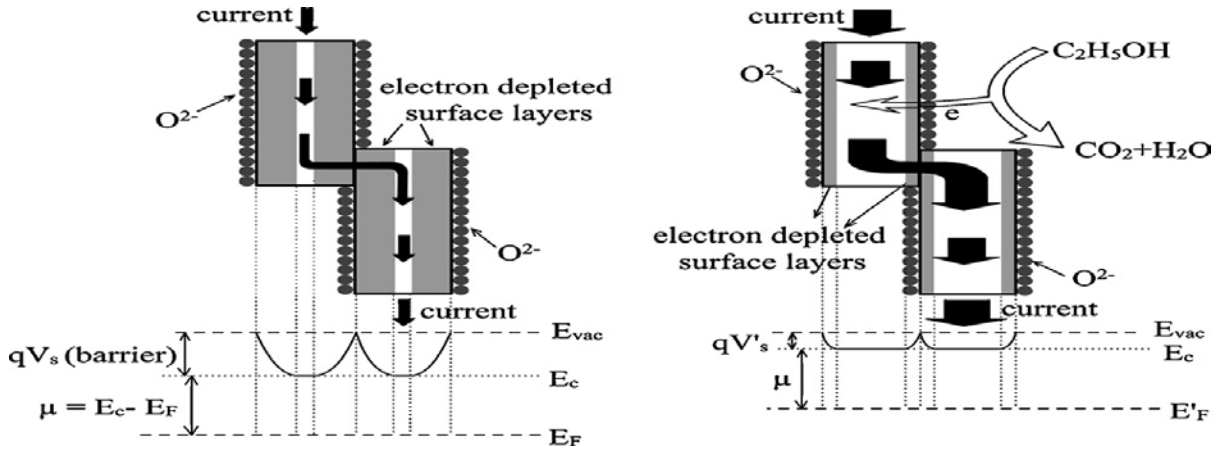

Figure 14. Schematic illustration of the mechanism of n-type materials.

The majority carriers in n-type Fe_2O_3 are electrons in the conduction band. When exposed to the air, the atmospheric oxygen molecules are adsorbed on the surface of the functional material causing the depletion layer at the surface of the material. As a result the material shows high resistance. When exposed to C_2H_5OH, the interaction of C_2H_5OH with the surface chemisorbed O^{2-} takes place [19].

$$C_2H_5OH + O^{2-} \rightarrow CH_3CHO + H_2O + 2e^- \quad \cdots\cdots\cdots\cdots\cdots\cdots\cdots\cdots \quad (5)$$

$$CH_3CHO + 5O^{2-} \rightarrow 2CO_2 + 2H_2O + 10e^- \quad \cdots\cdots\cdots\cdots\cdots\cdots\cdots\cdots \quad (6)$$

Releasing electrons to the depletion layer and increasing the electrical conductance of the semiconductor decreases the resistance. The sensitivity to ethanol vapor is greatly promoted by basic oxides [20]. Being specific to the ethanol vapor, the sensing performance should be related to the oxidation of ethanol vapor.

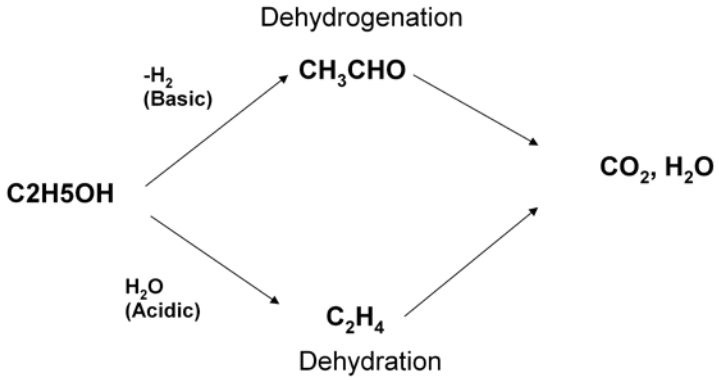

Figure 15. Routes of oxidzation of ethanol vapor.

As mentioned in Catalytic chemistry (Figure 15) ethanol vapor is oxidized via two reaction roots i.e. dehydrogenation to CH_3CHO on the basic surface and dehydration on the acidic surface. These intermediates are consecutively oxidized to CO_2 and H_2O:

V. CONCLUSION

To understand the effect of size of the particles of the test material that causes change in surface to volume ratio of the thick film on gas sensing performance thick film gas sensor nano Fe_2O_3

material films were prepared and studied. TEM images confirmed the nano size of the material and from diffractogram ring pattern the crystal nature of the material was confirmed. The gas sensing properties of the nano Fe_2o_3 film was studied. This study shows the higher sensitivity to ethanol gas at 350 ^oC temperature at 250 ppm gas concentration. The film is found highly selective to ethanol gas at 350 ^oC as compared to other gases tested. The quick response and moderate recovery times observed were 7s and 32 s.

ACKNOWLEDGEMENT

Author is thankful to BCUD, Pune University, UGC New Delhi for providing financial assistance for the project. Author is also thankful to Principal, K.A.A.N.M. Sonawane College, Satana and Principal, Arts, Commerce & Science College, Nandgaon for their valuable help during the project work. Author is thankful to SAIF, IIT, Mumbai for the help provided for characterization.

REFERENCES

[1] G.Telipan, The structure and gas sensing characteristics of γ-Fe_2O_3 semiconductor oxide, Proc. Int. Sym. Digital Earth, Sci Press, 1999, pp1-4,

[2] M.Ivanvokaya, D. Kosikau, G. Fagila, P. Nelli, Irkaev, Gas sensing properties of thin film hetrojunction structure based on Fe_2O_3 - In_2O_3 nanocompsites, Sens.Actuators B: Chem., Vol.93, 2003, pp. 422-430.

[3] O. K.Tan, W. Cao, W. Zhu, J. W. Chai, J. S. Pan, Ethanol sensor based on nanosized α-Fe_2O_3 with SnO_2, ZrO_2, TiO_2 solid solutions, Sens. Actuators B: Chem., Vol. 93, 2003, pp. 396-401.

[4] X.L. Gou, G.X. Wang, X.Y. Kong, D. Wexler, J. Horvat, J. Yang, J. Park, Flutelike Porous Hematite Nanorods and Branched Nanostructures: Synthesis, Characterization and Application for Gas-Sensing, Chem. Eur.J., Vol. 14, 2008, pp. 5996–6002.

[5] H. Liu, G.X. Wang, J. Park, J.Z. Wang, C. Zhang, Electrochemical performance of α-Fe_2O_3 nanorods as anode material for lithium-ion cells, Electrochim. Acta, Vol. 54, 2009, pp. 1733–1736.

[6] L. Chun, X.Z. Wu, X.M. Lou, Y.X. Zhang, Hematite nanoflakes as anode electrode materials for rechargeable lithium-ion batteries, Electrochim. Acta, Vol. 55, No. 9, 2010, pp. 3089–3092.

[7] J.G. Yu, X.X. Yu, B.B. Huang, X.Y. Zhang, Y. Dai, Hydrothermal synthesis and visible-light photocatalytic activity of novel cage-like ferric oxide hollow spheres, Cryst. Growth Des., Vol. 9, 2009, pp. 1474–1480.

[8] J.M. Gu, S.H. Li, E.B. Wang, Q.Y. Li, G.Y. Sun, R. Xu, H. Zhang, Single-crystalline α-Fe_2O_3 with hierarchical structures: Controllable synthesis, formation mechanism and photocatalytic properties, J. Solid State Chem., Vol. 182, No. 5, 2009, pp. 1265–1272.

[9] M.V. Reddy, T. Yu, C.H. Sow, Z.X. Shen, C.T. Lim, G.V.S. Rao, B.V.R. Chowdari, α-Fe_2O_3 Nanoflakes as an Anode Material for Li-Ion Batteries, Adv.Funct. Mater., Vol. 17, 2007, pp. 2792–2799.

[10] G. Korotcenkov, Metal oxides for solid stategas sensors:What determines our choice?, Material Science and Engineering B, Vol. 139, 2007, pp. 1-23.

[11] G. Kortcenkov, Gas response control through structural and chemical modification of metal oxides: State of the art and approaches, Senors and Actuators B, Vol. 107, No. 1, 2005, pp. 209-232.

[12] L. A. Patil, M. D. Shinde, A. R. Bari, V. V. Deo, D. M. Patil, M. P. Kaushik, Fe_2O_3 modified thick films of nanostructured SnO_2 powder consisting of hollow microspheres synthesized from pyrolysis of ultrasonically atomized aerosol for LPG sensing Sensors and Actuators B 155 (2011) 174–182.

[13] V. B. Patil, G.S. Shahane, L.P.Deshmukh, Material Chemistry and Physics 80(2003) 625-631

[14] G. E Patil, D. D. Kajale, V. B. Gaikwad and G. H. Jain, Nanocrystalline Tin Oxide Thin Film as a Low Level H_2S Gas Sensor, International Journal of Nanoscience, Vol. 10, No. 4, 2011, pp. 1-5.

[15] N. K. Pawar and G. H. Jain, Proceedings of 5th International Conference on Sensing Technology, ICST 2011, Study of nano Fe_2O_3 MOS thick films as ethanol gas sensor (2011), pp. 121-124.

[16] S. D. Shinde, G. E. Patil, D. D. Kajale, V. B. Gaikwad and G. H. Jain, Synthesis of ZnO nanorods by hydrothermal method for gas sensor applications, International Journal on Smart Sensing and Intelligent System, Vol. 5, No. 1, March 2012, pp. 57-70.

[17] S. D. Shinde, G. E. Patil, D. D. Kajale, V. G. Wagh, V. B. Gaikwad and G. H. Jain, Effect of annealing on gas sensing performance of nanostructured ZnO thick film resistors, International Journal on Smart Sensing and Intelligent System, Vol. 5, No. 1, March 2012, pp. 277-294.

[18] Huitao Fan, Tong Zhang, Xiujuan Xu, Ning Lv, Fabrication of N-type Fe2O3 and P-type LaFeO3 nanobelts by electrospinning and determination of gas-sensing properties Sensors and Actuators B 153 (2011) 83–88.

[19] M. Ivanovskaya, D. Kotsikau, G. Faglia, P. Nelli, Influence of chemical composition and structural factors of Fe_2O_3/In_2O_3 sensors on their electivity andsensor response to ethanol Sens. Actuators B 96 (2003) 498−503.

[20] Tomoki Maekawa,Jun Tamaki, Norio Miura and Noboru Yamazu, Development of SnO_2-based ethanol gas sensor, Sensors and Actuators B, Vol. 9, 1992, pp. 63-69.